Microelectronics Reliability 55 (2015) 1280–1284

Contents lists available at ScienceDirect

Microelectronics Reliability

journal homepage: www.elsevier.com/locate/mr

Robust prognostics for state of health estimation of lithium-ion batteries based on an improved PSO–SVR model

Taichun Qin [a], Shengkui Zeng [a,b], Jianbin Guo [a,b,*]

[a] School of Reliability and Systems Engineering, Beihang University, Beijing 100191, China
[b] Science and Technology on Reliability and Environmental Engineering Laboratory, Beijing 100191, China

ARTICLE INFO

Article history:
Received 25 May 2015
Received in revised form 21 June 2015
Accepted 29 June 2015
Available online 11 July 2015

Keywords:
Lithium-ion battery
Prognostic
State of health
Support vector regression
Particle swarm optimization

ABSTRACT

State of health (SOH) estimation of lithium-ion batteries is significant for safe and lifetime-optimized operation. In this study, support vector regression (SVR) is employed in battery SOH prognostics, and particle swarm optimization (PSO) is employed in obtaining the SVR kernel parameter. Through a new validation method, the proposed PSO–SVR model in this paper can well grasp the global degradation trend of SOH and is little affected by local regeneration and fluctuations. The case study shows that compared with the eight published methods, the proposed model can obtain more accurate SOH prediction results. Even SOH prediction starts from the cycle near capacity regeneration, the proposed model still can grasp the global degradation trend. Furthermore, the improved PSO–SVR model has great robustness when the training data contain noise and measurement outliers, which makes it possible to get satisfactory prediction performance without pre-processing the data manually.

1. Introduction

With the advantages of high energy density and lightweight, lithium-ion batteries are widely used in various kinds of portable devices, electric cars, spacecraft, etc. [1,2]. It is useful to accurately estimate state of charge (SOC) and state of health (SOH), as they play important roles in safe and reliable usage of lithium-ion batteries [3,4]. However, compared to the relatively mature study on SOC issue, SOH research still stays in the initial stage [5,6].

In general, the material properties and manufacturing assemblies are various from battery to battery [7]. Also, the performance of lithium-ion batteries degrades with many factors, such as environment temperature, and charging and discharging current, depth of discharge [3,8]. Moreover, it is rather difficult to measure parameters of the electrochemical reaction of lithium-ion batteries [4]. Therefore, SOH prognostics of data-driven approach seem more applicable than those of physical-model approach. In recent years, many algorithms based on data-driven approach have been applied to SOH prognostics, such as extended Kalman filter (EKF) [9], particle filtering (PF) [5], fuzzy logic [10], neural networks [11], and regressions [12]. However, with poor robustness, these algorithms are not good at dealing with limited data that contain uncertain information. As prediction errors are accumulating over time, these algorithms cannot be flexibly used in long-term prediction.

The battery capacity can be easily obtained and has a clear physical meaning [13], so capacity becomes the most common used health indicator of batteries. However, the uncertainty of capacity time series, generated by capacity regeneration [14], unexpected fluctuations, measurement error and other factors [7], is a big challenge for battery SOH prognostics. Olivares [15] has detected and isolated the effect of regeneration phenomena within the life-cycle model through a particle-filtering-based prognostics framework. Treating regeneration as a cycle process, Liu [14] has described capacity regeneration and degradation by using combination Gaussian progress function regression. With wavelet analysis, He [16] has separated local regeneration and fluctuation characteristics from global degradation characteristic, which makes it possible to analyze the two characteristics respectively. However, how to obtain accurate global degradation prediction of SOH with raw capacity data is still a topic that is worth studying.

In this paper, based on particle swarm optimization (PSO), a new approach to the optimal selection of support vector regression (SVR) parameters is proposed. This PSO–SVR model can well grasp the global degradation trend, despite the fact that the capacity time series contain regeneration, fluctuations, noise and outliers.

* Corresponding author at: School of Reliability and Systems Engineering, Beihang University, Beijing 100191, China.

http://dx.doi.org/10.1016/j.microrel.2015.06.133
0026-2714/

2. Methods

2.1. Support vector regression

ε-SVR is one of the most common used SVR models [17]. When the dataset $\{x_i, y_i\}$ presents a linear relationship, the regression function can be given by:

$$f(\mathbf{x}) = \mathbf{w}\phi(\mathbf{x}) + b \tag{1}$$

where $\boldsymbol{w}$ and b denote the undetermined parameters.

The optimization object can be expressed as [18]:

$$\min \frac{1}{2}\|\mathbf{w}\|^2 + C\sum_{i=1}^{n}(\xi_i + \xi_i^*) \tag{2}$$

$$\text{s.t.}\begin{cases} y_i - \mathbf{w}\phi(\mathbf{x}_i) - b \le \varepsilon + \xi_i \\ -y_i + \mathbf{w}\phi(\mathbf{x}_i) + b \le \varepsilon + \xi_i^*, \quad i = 1,2,\cdots,n \\ \xi_i, \xi_i^* \ge 0 \end{cases} \tag{3}$$

where ε is the width of ε-tube, constant C (positive) is the penalty degree of the sample whose error is larger than ε, and slack variables ξ_i and ξ_i^* are the distances between actual values and the nearer boundary of ε-tube.

For nonlinear cases, they can be converted into linear cases though kernel functions. The radial basis function (RBF) kernel is used in this paper:

$$K(\mathbf{x}_i, \mathbf{x}_j) = \exp\left(-\frac{1}{2}\left(\frac{\|\mathbf{x}_i - \mathbf{x}_j\|}{\sigma}\right)^2\right) \tag{4}$$

where σ is the parameter of RBF.

2.2. Particle swarm optimization

PSO was proposed by Kennedy and Eberhart in 1995 [19]. Its basic idea is to obtain the optimal solution (also called particle) by minimizing a fitness function. The velocity and place of every particle will be updated by [20,21]:

$$v_i^{k+1} = wv_i^k + c_1 r_1\left(pbest_i^k - x_i^k\right) + c_2 r_2\left(gbest^k - x_i^k\right) \tag{5}$$

$$x_i^{k+1} = x_i^k + v_i^{k+1} \tag{6}$$

where
v_i^k denotes the velocity of particle i at iteration k, x_i^k denotes the place of particle i at iteration k, $pbest_i^k$ is the optimal solution (individual optimal solution) of particle i until kth iteration, $gbest^k$ is global optimal solution of all particles until kth iteration, w denotes inertia weight coefficient, r_1 and r_2 are random numbers between 0 and 1, and c_1 and c_2 are positive acceleration constants.

2.3. Improved PSO–SVR

From Eqs. (2), (3) and (4), the parameters ε, C and σ need to be determined when we use ε-SVR model for nonlinear regression. Among them, both ε (the width of ε-tube) and C (the penalty degree of samples) have clear statistical meanings. They can reflect the commonality of the same type batteries and can be determined based on experience. On the other hand, nuclear parameter σ does not have a definite meaning, and it can reflect the individuality of different batteries. As a result, we expect to obtain an appropriate value of σ for each battery through PSO algorithm based on its earlier capacity time series.

An appropriate criterion is important to evaluate the fitting (or prediction) performance with different values of the nuclear parameter. Among the criteria, mean squared error (*MSE*) is the most widely used one. However, *MSE* cannot directly describe the correlation of the fitting (or prediction) curve and the actual SOH curve. Therefore, in this paper, a weighted sum of *MSE* and coefficient of determination (denoted by R^2) is chosen as the criterion to evaluate the fitting (or prediction) effects. The weighted sum of *MSE* and R^2 is denoted by *MC*, where *MSE*, R^2 and *MC* are shown as:

$$MSE = \frac{1}{N}\sum_{i=1}^{N}(f(x_i) - y_i)^2 \tag{7}$$

$$R^2 = \frac{\left(N\sum_{i=1}^{N} f(x_i)y_i - \sum_{i=1}^{N} f(x_i)\sum_{i=1}^{N} y_i\right)^2}{\left(N\sum_{i=1}^{N} f(x_i)^2 - \left(\sum_{i=1}^{N} f(x_i)\right)^2\right)\left(N\sum_{i=1}^{N} y_i^2 - \left(\sum_{i=1}^{N} y_i\right)^2\right)} \tag{8}$$

$$MC = MSE - aR^2 \tag{9}$$

where a is a *MSE* and R^2.

During the training stage, model validation is required to obtain the optimal value of the model parameter. In k-fold cross-validation, the most commonly used validation, the dataset (training samples) $\mathcal{D}$ is randomly split into k mutually exclusive subsets $\mathcal{D}_1, \mathcal{D}_2, \ldots, \mathcal{D}_k$. The model is trained and tested k times. In each time, it is trained on $\mathcal{D} \setminus \mathcal{D}_i$ and tested on $\mathcal{D}_i$, where $i \in \{1,2,\ldots,k\}$. The output of cross-validation is the average of all the k testing errors.

SOH prognostics focus on predicting future degradation trend of lithium-ion batteries by using earlier degradation time series. Therefore, k-fold cross-validation that treats all training samples equally seems not very reasonable. A new validation method is shown in Fig. 1. In this validation method, the model is tested on all the training samples (dataset $\mathcal{D}$) rather than on the subset $\mathcal{D}_i$. It is to ensure that the good performance of the model in the prediction stage is due to the good grasping of the degradation trend in the training stage rather than by accident.

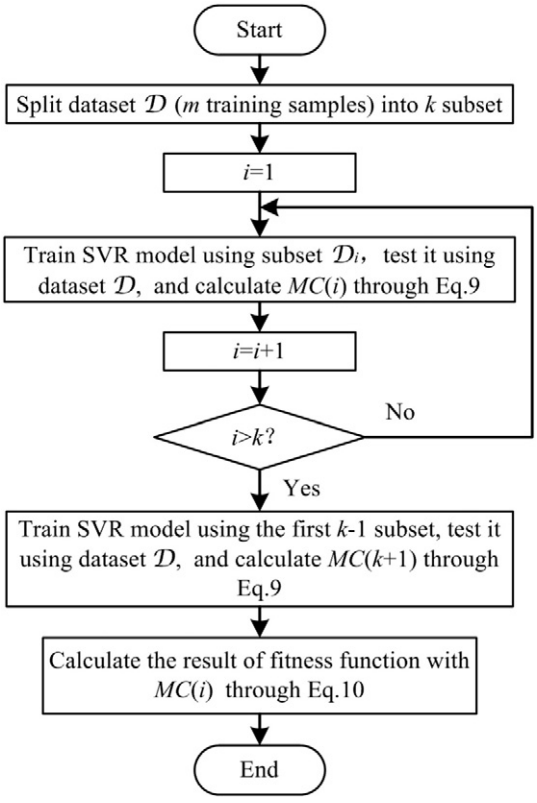

Fig. 1. The flowchart of improved validation method.

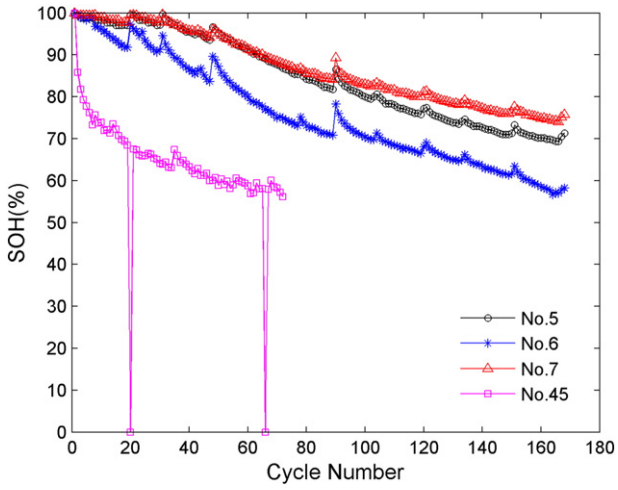

Fig. 2. SOH values of batteries Nos. 5–7 and No. 45.

The fitness function is described as Eq. (10) and F is the output:

$$F = \frac{1}{2k}\left(\sum_{i=1}^{k} MC(i) + kMC(k+1)\right). \tag{10}$$

The fitness function is the weighted average of two parts. In the first part, a small number of training samples are used in each cycle to make the model able for long-term extrapolation. In the second part, the first (k-1) parts of the training samples are used to make the model have the ability of backward extrapolation. Moreover, the multiplication factor k in the second part is to balance the effects of the two parts. The smaller the value of F is, the better the performance of the SVR model is.

The steps of the improved PSO–SVR are briefly described as follows:

Step 1: Take first m training data from a total of M.

Step 2: Obtain the optimal value of parameter σ by PSO. The validation process (Fig. 1) is nested in the PSO algorithm. Specifically, the fitness function (Eq. (10)) is the optimization objective of PSO and the values of parameter σ are given by every loop of PSO.

Step 3: Assign the optimal value to σ, and train the SVR model using first m samples.

Step 4: Use the trained model to predict the future degradation of batteries, and use the last (M–m) data to evaluate the prediction performance.

3. Experiments and analysis

3.1. Raw data of lithium-ion batteries

The lithium-ion battery degradation experiment data involved in this paper are from NASA Ames Prognostics Center of Excellence (PCoE) [22]. The 18650 sized batteries (No. 5, No. 6, No. 7 and No. 45) were run under three different operational conditions (charge, discharge and impedance) at temperature of 24 °C (No. 5, No. 6 and No. 7) or 4 °C (No. 45). Charging current was constant with a level of 1.5A until the battery voltage achieved 4.2 V. Then the batteries were continued in a constant voltage mode until the charge current fell to 20 mA. For batteries No. 5, No. 6 and No. 7, discharge was run at a constant current level of 2A until the battery voltage dropped to 2.7 V, 2.5 V and 2.2 V respectively. For battery No. 45, discharge current level was 1A until the battery voltage dropped to 2 V.

In this paper, the capacity is used to describe battery SOH. The definition is shown as:

$$\mathrm{SOH} = \frac{C_i}{C_0} \times 100\% \tag{11}$$

where C_i is the capacity at ith degradation cycle and C_0 is the initial capacity. The SOH values of four batteries are shown in Fig. 2.

3.2. Comparison and analysis of prediction performance

In this paper, batteries Nos. 5–7 are used to illustrate the effectiveness of the improved PSO–SVR model. The capacity degeneration data from cycle 1 to cycle 100 are selected as the training samples to predict the future SOH values, while the data from cycle 101 to cycle 168 are selected for evaluating the prediction performance of the improved PSO–SVR. The training data number and prediction data number are the same as Ref. [14] and Ref. [16], which is helpful for performance comparisons among different prediction methods. Table 1 shows the prediction errors of the improved PSO–SVR and eight published methods (five methods from Ref. [14] and three from Ref. [16]) on batteries Nos. 5–7. Two criteria, mean absolute percentage error (MAPE) and root mean square error (RMSE), are adopted to evaluate the prediction performance of different methods:

$$\mathrm{MAPE} = \frac{1}{N}\sum_{i=1}^{N}\left|\frac{y_i - \hat{y}_i}{y_i}\right| \times 100\% \tag{12}$$

$$\mathrm{RMSE} = \sqrt{\frac{1}{N}\sum_{i=1}^{N}(y_i - \hat{y}_i)^2}. \tag{13}$$

From Table 1, we can see that the improved PSO–SVR method has much better prediction performance than the eight published methods. Among the eight published methods, SE–MGPR has the best prediction results. Both its predictions MAPE and RMSE are the smallest on batteries Nos. 5–7. Therefore, the smallest prediction MAPE and RMSE of the eight published methods on battery No. 5 are 1.38% and 1.20 respectively, while the prediction MAPE and RMSE of the improved PSO–SVR are 0.82% and 0.75 respectively. In the same way, we found that the prediction MAPE and RMSE of the improved PSO–SVR on battery No. 6 are also the smallest. The prediction RMSE of the improved PSO–SVR on battery No. 7 is smaller than that of SE–MGPR, although the prediction MAPE is equal. By comparison, it can be concluded that the improved PSO–SVR could effectively improve the prediction performance of battery SOH. That is mainly because the improved PSO–SVR focuses on

Table 1
Performance comparisons of different methods for Nos. 5, 6 and 7.

Battery No.	Error criteria	Basic GPR[a]	LGPFR[a]	QGPFR[a]	CLGPFR[a]	CQGPFR[a]	SMK–GPR[b]	P–MGPR[b]	SE–MGPR[b]	Improved PSO–SVR
5	MAPE (%)	12.10	23.0	1.90	1.60	2.10	1.65	1.55	1.38	0.82
	RMSE	13.03	1.71	1.50	1.36	1.80	1.38	1.36	1.20	0.75
6	MAPE (%)	27.0	10.30	7.70	10.20	29.0	10.60	2.96	2.93	2.28
	RMSE	22.51	6.90	5.12	6.86	20.44	7.08	2.12	2.11	1.66
7	MAPE (%)	19.20	1.90	5.40	1.70	2.60	1.91	1.09	1.02	1.02
	RMSE	20.70	1.59	5.52	1.73	2.69	1.88	1.14	1.07	0.97

[a] Results of these methods are obtained from reference [14].
[b] Results of these methods are obtained from reference [16].

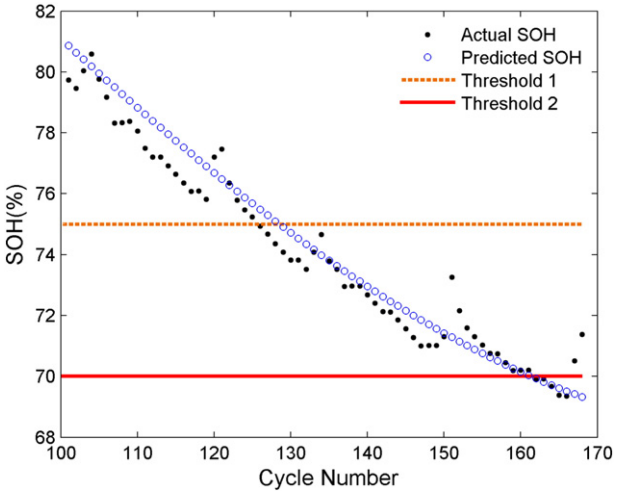

Fig. 3. SOH prognostics based on improved PSO–SVR.

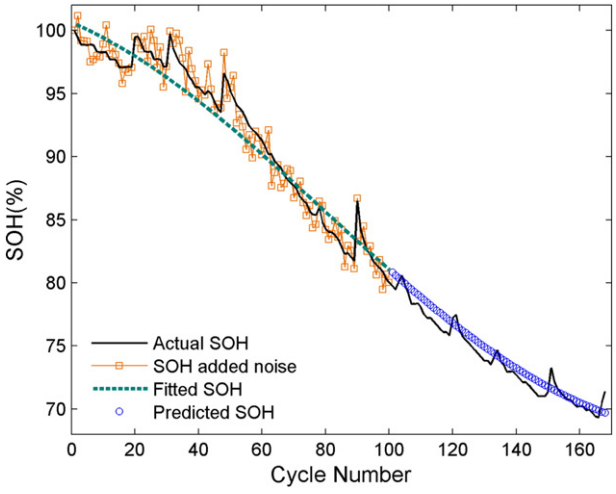

Fig. 5. SOH prognostics with noise.

grasping the global trend of capacity degradation rather than capturing the local regeneration and fluctuations.

Take battery No. 5 as an example; the SOH prediction results after cycle 100 are shown in Fig. 3. It can be seen that the prediction values of the improved PSO–SVR are close to the actual SOH values. Therefore, after giving a fault threshold, the remaining useful life (RUL) can be obtained. For different devices, the fault thresholds of batteries may be different but generally vary from 70% to 80% of the initial SOH [6]. Taking 70% and 75% for example, as shown in Fig. 3, the prediction errors of RUL are 3 cycles and 0 respectively. Moreover, the largest prediction error is only 6 cycles. The excellent prediction performance indicates that the improved PSO–SVR can be well applied to RUL prediction under different fault thresholds.

3.3. The effect of capacity regeneration

Still for battery No. 5, as seen in Fig. 2, the most noticeable regeneration is after the 89th cycle, which makes the capacities from the 90th cycle to the 95th cycle no lower than the 89th cycle. Therefore, three sets of training data are selected to analyze the influence of regeneration. The numbers of training data are 89 (from cycle 1 to cycle 89), 95 and 100 respectively. Fig. 4 shows the SOH prediction results under the above three situations, and the results around cycle 160 are enlarged and given in the upper right of Fig. 4. It can be seen from the three prediction curves in the enlarged figure that the SOH prediction results have small differences (only one or two cycles). In addition, the prediction MAPE are 0.89%, 0.88% and 0.82% respectively and the prediction RMSE are 0.82, 0.77 and 0.75 respectively. The close errors under three situations demonstrate that regeneration has small influence on the prediction accuracy of the improved PSO–SVR.

3.4. Robustness analysis

The training data usually contain some unexpected errors, and their values are generally random [7]. In order to analyze the anti-noise performance of the improved PSO–SVR, a Gaussian noise is added to the raw capacity samples of battery No. 5. Fig. 5 shows the training data with noise and SOH prediction results. Through calculating the prediction errors from cycle 101 to cycle 168, the prediction MAPE and RMS on battery No. 5 are 0.97% and 0.81 respectively. They are close to 0.82% and 0.75, which are the prediction errors with raw data and can be read from the last row of Table 1. This means that the improved PSO–SVR can achieve relatively accurate SOH prediction results under some noise conditions.

Battery No. 45 is selected to analyze the robustness of the improved PSO–SVR because its raw capacity data contain outliers. As shown in Fig. 6, the two outliers are at cycle 20 and cycle 66. SOH prediction

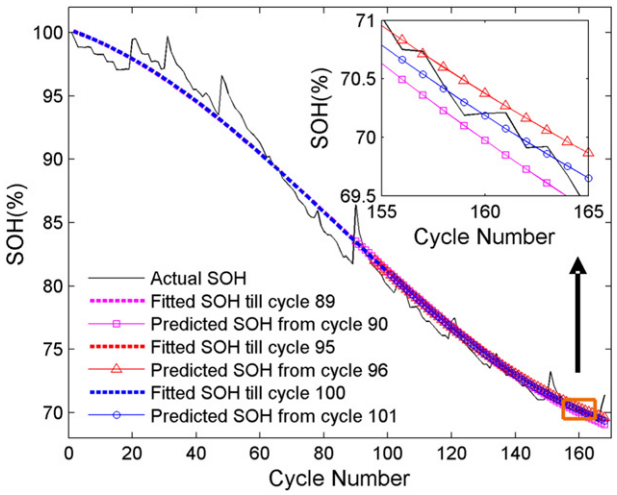

Fig. 4. SOH prognostics affected by regeneration.

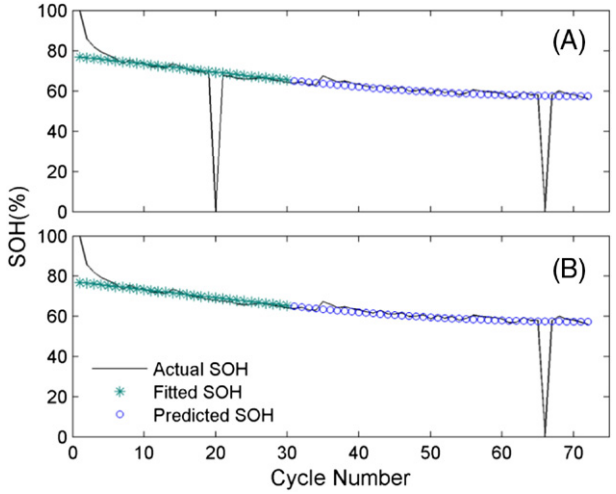

Fig. 6. SOH prediction on battery No. 45: (A) with outlier; (B) eliminated outlier.

Table 2
The cycle number corresponding to each outlier.

Outlier	1	2	3	4	5	6	7	8	9	10
Cycle number	20	10	17	21	24	13	3	30	22	1
Outlier	11	12	13	14	15	16	17	18	19	20
Cycle number	19	4	27	25	9	23	8	7	14	29
Outlier	21	22	23	24	25	26	27	28	29	30
Cycle number	12	28	5	6	11	2	15	18	26	16

results using 30 raw SOH data (from cycle 1 to cycle 30) as the training samples are shown in Fig. 6(A). By contrast, the prediction results after eliminating the outlier at cycle 20 are shown in Fig. 6(B). The outlier is replaced by the mean value of its two adjacent samples, which is the most common method of eliminating outliers [6]. From Fig. 6(A) and (B), it is clear that the two sets of prediction results after cycle 30 are almost the same. In other words, the improved PSO–SVR can get high accuracy prediction results without eliminating the outliers manually.

Moreover, the effect of the amount of outliers is thoroughly investigated. Still take the first 30 SOH data of battery No. 45 as the training samples, but the difference is that more outliers are added into the raw SOH data. The corresponding cycle numbers of the randomly produced outliers are shown in Table 2 and the values of SOH at these cycles are replaced by zero. The outliers are added into the SOH time series one by one to analyze the robustness of the improved model. With the increase in the amount of the outliers, the changes of the prediction MAPE and RMSE are shown in Fig. 7. The prediction errors remain stable when there are no more than six outliers (20% of the training samples). In this case, the prediction MAPE is around 1.6% and the prediction RMSE is about 1.2. With some fluctuations, prediction errors gradually increase to 3.2% (MAPE) and 2.2 (RMSE) when the amount of the outliers increases to fourteen. Then, the prediction MAPE jumps to 48% and the prediction RMSE soars to 29 when there are fifteen outliers (50% of the training samples). After that, the prediction errors reach the highest level at about 99% (MAPE) and 60 (RMSE). Actually, there may be some outliers in the training samples, but the amount is unlikely to exceed 20%. Therefore, the prediction errors of the improved model are stable and small in most cases. It indicated that the improved model has excellent robustness and can be well applied to SOH prognostics when the training samples contain some outliers.

4. Conclusion

To obtain more accurate long-term prediction results of SOH with limited raw capacity data, we have proposed an improved PSO–SVR model. This model was aimed at grasping the global degradation trend without focusing on local fluctuations. The criterion composed of *MSE* and R^2 was used to evaluate the performance from two different angles in the parameter optimization process. A fitness function for PSO and a new validation method were proposed to make the model have the ability to grasp the global degradation trend and realize long-term backward extrapolation.

Case studies were carried out to evaluate the performance of the proposed model. The results showed that: 1) using the previous capacity data of the current battery, this model can achieve more accurate SOH prognostics; 2) this model can get satisfactory results of RUL estimation under different fault thresholds; 3) even starting from the cycle near capacity regeneration, this model can also have good prediction performance; and 4) this model has great robustness and can get accurate prediction results when the data contain noise and outliers.

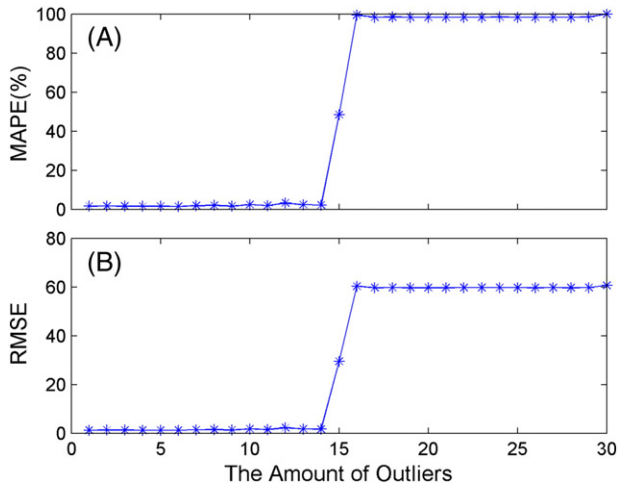

Fig. 7. Errors with different amounts of outliers.

Acknowledgments

This work was supported by the National Natural Science Foundation of China (NSFC: 61304218) and Beijing Higher Education Young Elite Teacher Project (YETP1123).

References

[1] J.G. Kim, B. Son, S. Mukherjee, N. Schuppert, A. Bates, O. Kwon, et al., A review of lithium and non-lithium based solid state batteries, J. Power Sources 282 (2015) 299–322.
[2] Y. Sone, Charge/discharge performance of lithium-ion secondary cells under microgravity conditions: lessons learned from operation of interplanetary spacecraft Hayabusa, Electrochim. Acta 100 (2013) 358–363.
[3] S.M. Rezvanizaniani, Z. Liu, Y. Chen, J. Lee, Review and recent advances in battery health monitoring and prognostics technologies for electric vehicle (EV) safety and mobility, J. Power Sources 256 (2014) 110–124.
[4] L.X. Liao, F. Kottig, Review of hybrid prognostics approaches for remaining useful life prediction of engineered systems, and an application to battery life prediction, IEEE Trans. Reliab. 63 (1) (2014) 191–207.
[5] B. Saha, K. Goebel, S. Poll, J. Christophersen, Prognostics methods for battery health monitoring using a Bayesian framework, IEEE Trans. Instrum. Meas. 58 (2) (2009) 291–296.
[6] S.S.Y. Ng, Y. Xing, K.L. Tsui, A naive Bayes model for robust remaining useful life prediction of lithium-ion battery, Appl. Energy 118 (2014) 114–123.
[7] W. He, N. Williard, M. Osterman, M. Pecht, Prognostics of lithium-ion batteries based on Dempster–Shafer theory and the Bayesian Monte Carlo method, J. Power Sources 196 (23) (2011) 10314–10321.
[8] J. Zhang, J. Lee, A review on prognostics and health monitoring of Li-ion battery, J. Power Sources 196 (15) (2011) 6007–6014.
[9] G.L. Plett, Extended Kalman filtering for battery management systems of LiPB-based HEV battery packs, part 1–3, J. Power Sources 134 (2) (2004) 252–292.
[10] A.J. Salkind, C. Fennie, P. Singh, T. Atwater, D.E. Reisner, Determination of state-of-charge and state-of-health of batteries by fuzzy logic methodology, J. Power Sources 80 (1–2) (1999) 293–300.
[11] Q. Kejun, Z. Chengke, Y. Yue, M. Allan, Temperature effect on electric vehicle battery cycle life in Vehicle-to-grid applications, China International Conference on Electricity Distribution (CICED) 2010, pp. 1–6.
[12] B. Pattipati, K. Pattipati, J.P. Christopherson, S.M. Namburu, D.V. Prokhorov, Q. Liu, Automotive battery management systems, IEEE Autotestcon 2008, pp. 581–586.
[13] G. Jin, D.E. Matthews, Z. Zhou, A Bayesian framework for on-line degradation assessment and residual life prediction of secondary batteries in spacecraft, Reliab. Eng. Syst. Saf. 113 (2013) 7–20.
[14] D. Liu, J. Pang, J. Zhou, Y. Peng, M. Pecht, Prognostics for state of health estimation of lithium-ion batteries based on combination Gaussian process functional regression, Microelectron. Reliab. 53 (6) (2013) 832–839.
[15] B.E. Olivares, M.A. Cerda Munoz, M.E. Orchard, J.F. Silva, Particle-filtering-based prognosis framework for energy storage devices with a statistical characterization of state-of-health regeneration phenomena, IEEE Trans. Instrum. Meas. 62 (2) (2013) 364–376.
[16] Y. He, J. Shen, J. Shen, Z. Ma, State of health estimation of lithium-ion batteries: a multiscale Gaussian process regression modeling approach, AICHE J. 61 (5) (2015) 1589–1600.
[17] S.F. Fang, M.P. Wang, W.H. Qi, F. Zheng, Hybrid genetic algorithms and support vector regression in forecasting atmospheric corrosion of metallic materials, Comput. Mater. Sci. 44 (2) (2008) 647–655.
[18] H. Drucker, C.J.C. Burges, L. Kaufman, A. Smola, V. Vapnik, Support vector regression machines, 10th Annual Conference on Neural Information Processing Systems (NIPS) 1997, pp. 155–161.
[19] J. Kennedy, R. Eberhart, Particle swarm optimization, IEEE International Conference on, Neural Networks, vol. 4 1995, pp. 1942–1948.
[20] I.C. Trelea, The particle swarm optimization algorithm: convergence analysis and parameter selection, Inf. Process. Lett. 85 (6) (2003) 317–325.
[21] B. Long, W. Xian, L. Jiang, Z. Liu, An improved autoregressive model by particle swarm optimization for prognostics of lithium-ion batteries, Microelectron. Reliab. 53 (6) (2013) 821–831.
[22] B. Saha, K. Goebel, Battery data set, NASA Ames Prognostics Data Repository. , NASA Ames, Moffett Field, CA, 2007. (http://ti.arc.nasa.gov/project/prognostic-data-repository).